Forecasting the Ionospheric f0F2 Parameter One Hour in Advance Using Recurrent Neural Network

Zhe Lv[a], Changjun Yu[b] and Aijun Liu[c]
Harbin Institute of Technology Weihai, China.
[a]lvzhehit@126.com, [b]yuchangjun@hit.edu.cn, [c]liuaijun@hit.edu.cn

Abstract. It is difficult to forecast the state of ionosphere because the time-varying characteristics. Using recurrent neural network (RNN) one hour ahead prediction of the critical parameter of ionospheric F2 layer (f0F2) is realized. The prediction model is developed based on 11 years (from 2005 to 2016) of data measured from ionospheric vertical stations in China. By analyzing time series correlation of f0F2 and solar-terrestrial and geomagnetic activities, several parameters are selected as inputs. Though training the RNN model, the forecasting values one hour ahead can be obtained. For this time-series problem, the predicted ability of RNN is better than Artificial Neural Network (ANN) and the autocorrelation method by comparing the results of three different algorithms.

Keywords: Ionospheric critical frequency, modeling and forecasting, recurrent neural networks.

1. Introduction

Due to the time-varying and dispersive characteristics of the ionosphere, communication systems cannot just be evaluated by the fixed factors, especially for the high frequency radars and shortwave communication systems, the working parameters must be adaptively adjusted according to the current state of the ionosphere. The f0F2 is one of the most important parameters for quantifying the plasma density variability of the ionosphere. Much work has been done in forecasting the f0F2 on different time scales, mostly in 1 hour or 24 hours ahead.

Because of the nonlinear characteristics of the ionosphere, artificial neural networks (ANN) are very encouraging in the prediction. No matter how long the forecasting time in advance, it is the key to construct the relationship between inputs and outputs sensibly. In the context of forecasting the f0F2 one hour in advance, ANN was used for the first time by Altinay [1], and a training strategy in order to significantly enhance the generalization or extrapolation ability of ANN is adopted. Meanwhile, a method for determining the relative significant of ANN inputs was developed. Kumluca [2] introduced another method also based on ANNS, and it was the application of neural networks for modeling both temporal and spatial dependencies. Williscroft [3] used ANN to forecast the the noon values of f0F2. The prediction of monthly median f0F2 values by Lamming, the short-time forecasting by Cander and modeling of day variations of f0F2 by Francis all have been in relation with artificial-neural network-based methods [4] [5] [6]. With the development of machine learning, Chen introduced a method for forecasting the f0F2 using the support vector machine (SVM) approach [7] [8], and Sai Gowtam presented a method combined artificial neural networks and global GPS dataset [9]. Feynman and Gabriel proposed that variations in the solar, magneto spheric and ionospheric characteristics could affect a variety of ground-based and space-borne technological systems [10]. The methods trying to involve an auto-correlation [11], the multi-linear-regression method [12] and the data-assimilation method [13] have one thing in common that they use past f0F2 values as an input. Koutroumbas introduced an one-step ahead prediction using time series forecasting techniques [14] and then the time series autoregression method was used for the ionospheric forecasting over Europe [15]. Some literatures utilized the autoregression method, Muhtarov proposed a correlated autoregression ionospheric model driven by a synthetic geomagnetical index [16], Tsagouri presented an autoregression model for ionospheric short-term forecast based on the solar wind [17] [18], Tsagouri and Belehaki combined an autoregression forecasting algorithm with the empirical storm-time model [19]. In order to study the effects of the

storm on the ionosphere, an empirical storm-time ionospheric correction model has been developed by Araujo Pradere [20] [21], and Ban introduced a forecasting model of low-latitude storm-time ionospheric f0F2 [22].

In recent years, benefitting from the computing capacity growth, deep learning has been widely used in various fields [23], and it also provides a new idea for predicting the critical frequency of ionosphere. As we know, some tasks require awareness of time dataset, such as image captioning, personal recommendation and speech synthesis. In other domains, like the nature language processing, a model must learn from time sequences [24]. In fact, the observations of ionospheric critical frequency are time sequences, too [25] [26]. In this paper, we chose a deep learning algorithm called recurrent neural network (RNN) to forecast f0F2. Recurrent neural networks use back-propagation (BP) to reduce losses, just like convolution neural network (CNN), but RNN can retain a state or memory, that reflects the relationship between the previous time node and the latter time node [27] [28], which is very important for time series analysis.

2. Proposed Method

Recurrent neural network is a popular variant of artificial neural network, which works really well on time sequential data types, i.e. a set of data points which are arranged in a particular order such that related data points follow each other. Fig. 1 shows the basic recurrent neural network structure, and it takes in both the sequence data input vector (x) and the hidden state information (a) and uses them to predict the sequence data output, and we unroll the RNN into a repetitive chain of cells which correspond to the length of the sequence data.

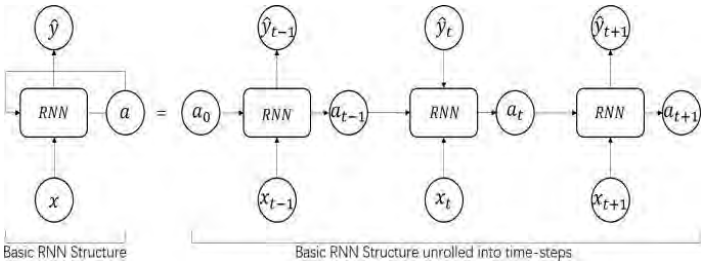

Fig. 1 Basic RNN structure and structure unrolled into time-steps

The internal structure in single RNN cell shows in Fig. 2, where x(t) is input at time-step(t), a(t-1) is hidden state activation at previous time-step(t-1), W_{ah} is hidden-to-hidden weight matrix, W_{xh} is input-to-hidden weight matrix, b_h is hidden state bias vector, W_{ao} is hidden-to-output weight matrix, b_o is output bias vector, ht is hidden state at time step(t), at is hidden state activation at time-step(t), o_t is predicted output at time-step(t), and $\hat{y}t$ is predicted output activation at time-step(t).

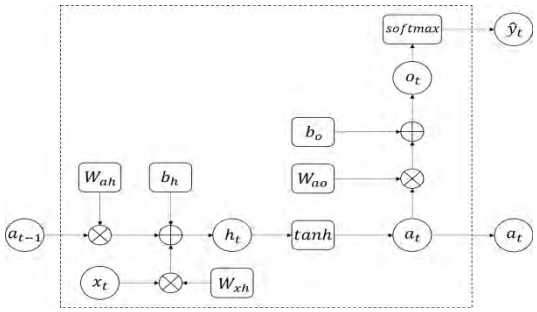

Fig. 2 One basic RNN cell.

The feedforward propagation of RNN can be expressed as:

$$h_t = (W_{xh} \times x_t) + (W_{ah} \times a_{(t-1)}) + b_n \quad (1)$$

$$a_t = tanh(h_t) \quad (2)$$

$$o_t = (W_{ao} \times a_t) + b_n \quad (3)$$

$$y_t = softmax(o_t) \tag{4}$$

The goal of back propagation though time (BPTT) in the RNN is to compute the partial derivatives of the weight matrices and bias vectors with respect to the final loss L. The loss function is defined for cost computation. In this case, the cross entropy loss function is used:

$$L_t = -\sum_{i}^{C} y_i^t log(\hat{y}_i^t) \tag{5}$$

And the following 5 equations are to update parameters:

$$\frac{\partial L_t}{\partial W_{ao}} = \sum_t \left(\frac{\partial L_t}{\partial o_t} \times a_t \right) \tag{6}$$

$$\frac{\partial L_t}{\partial b_o} = \sum_t \left(\frac{\partial L_t}{\partial o_t} \right) \tag{7}$$

$$\frac{\partial L_t}{\partial W_{ah}} = \sum_t \left(\frac{\partial L_t}{\partial h_t} \times x_t \right) \tag{8}$$

$$\frac{\partial L_t}{\partial W_{xh}} = \sum_t \left(\frac{\partial L_t}{\partial h_t} \times x_t \right) \tag{9}$$

$$\frac{\partial L_t}{\partial b_h} = \sum_t \left(\frac{\partial L_t}{\partial h_t} \right) \tag{10}$$

3. Data Set

For training the RNN model, several input parameters are introduced here. The appropriate input parameters are the key to the success of the experiment. And considering that RNN only has short term memory, some input parameters related to f0F2 are selected.

3.1 Input Related to f0F2.

The hourly values of f0F2 as train set were from the ionospheric vertical stations in China from 2004 to 2014, which were selected as the representation of solar maximum and minimum as a solar 11-year activity cycle, and the test set from 2015 and 2016 were used to test the forecast precision qualitatively. Five ionospheric stations were selected which located in Wuhan(WH), Hainan(HN), Urumqi(UQ), Guangzhou(GZ) and Beijing(BJ), and the main observations were shown in Table 1.

Table 1 Main Observations From Ionospheric Vertical Stations

Parameters	Names
Critical frequency of F2-layer(MHz)	f0F2
Peak height of F2-layer(km)	hmF2
Virtual height of F-layer(km)	hpF
Critical frequency of E-layer(MHz)	f0E
Minimum frequency receive(MHz)	M3000F2
Critical frequency of F1-layer(MHz)	f0F1
Critical frequency of Es-layer(MHz)	f0Es

The f0F2 is selected as one input for RNN of these eight parameters. Though the variant of f0F2 is the stochastic process, it is statistically related to diurnal and seasonal variations. The typical variations of f0F2 are illustrated in Figure 3. The f0F2 values for the ionospheric station Wuhan in 0.1MHz are plotted for the week after the vernal equinox in 2016. The f0F2 values are minimum at midnight and maximum at midday. From Figure 3(a), it is obvious that the f0F2 values are the diurnal variations. Then, the monthly mean values of f0F2 are demonstrated in Figure 3(b). The monthly median values for January 2014 to December 2016 are plotted, and the seasonal variations are very apparent from one month to another.

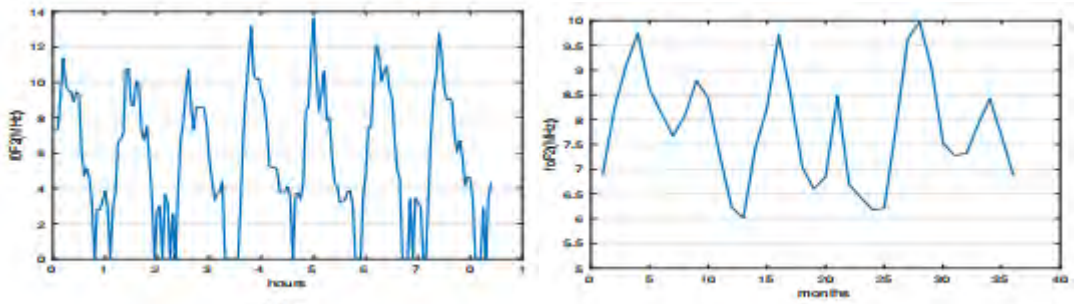

(a) (b)

Fig. 3 (a) Diurnal variations of f0F2. (b) Seasonal variations of f0F2

Considering that the f0F2 values themselves should be meaningful in forecasting the hourly prediction in advance, the present value of f0F2 is fed to the RNN and several derivatives of f0F2 are also considered. If the f0F2 to be forecast is at time t+1, the related inputs can be expressed as follows:

• Present observation of f0F2: f(t)
• The first increments of f0F2: df(t) = f0F2(t)-f0F2(t-1)
• The second increments of f0F2:ddf(t)=df(t)-df(t-1)

And reconsidering the correlation in statistics, the present value of f0F2 could have high coefficient with the previous values. Assume that the sequence of observations within a day is :

$$f(n) = \{f(t_0), f(t_1), ..., f(t_m)\}, m = 0, 1, ...23 \tag{11}$$

The corresponding average sequence of Equation 11 is:

$$\overline{f(n)} = \left\{\overline{f(t_0)}, \overline{f(t_1)}, ..., \overline{f(t_m)}\right\}, m = 0, 1, ...23 \tag{12}$$

Where:

$$\overline{f(n)} = \frac{1}{N+1}\sum_{k=0}^{N} f(t_{m-k}), N = 0, 1, ..., 23 \tag{13}$$

Then we considered the coefficient between the current values and mean values in the previous 30 days.Assume that the sequence of observations within 30 days is:

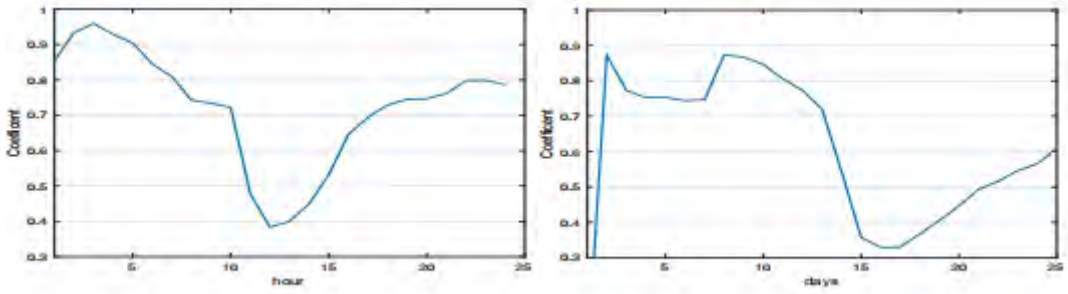

(a) (b)

Fig. 4 (a) The Coefficient of the Present and 24 Hours Early. (b) The Coefficient of the Present and 30 Days Early

$$f(n) = \{f(t_0), f(t-1), ..., f(t-m)\}, m = 1, 2, ..., 30 \tag{14}$$

Similarly,

$$\overline{f(n)} = \left\{\overline{f(t_0)}, \overline{f(t_1)}, ...\overline{f(t_m)}\right\}, m = 1, 2, ..., 30 \tag{15}$$

Where:

$$\overline{f(n)} = \frac{1}{N}\sum_{k=0}^{N} f(t), N = 1, 2, ..., 30 \tag{16}$$

In Figure 4, the coefficients of Equation (11)(12) and Equation (14)(15) are plotted respectively. It can be found that the present value of f0F2 is highly related with the average value from 3 hours early

in Figure 4(a) and in Figure 4(b) it can be found that the present value of f0F2 is related to both the average value from the previous day and a week early.
So the following parameters are also selected as inputs:

• The mean of f0F2 from previous 3 hours: $\frac{1}{3}\sum_{i=1}^{3} f(t_{n-i})$
• The mean of f0F2 from the previous day and a week early: f0F2(d-1) and f0F2(d-7)

3.2 Diurnal and Seasonal Variation.

Due to the complex of the ionosphere, the predicted accuracy and practicability would not be satisfied if only the present observation and the inputs with f0F2. The reason is that the characterizations of the influence factors leading to the ionospheric changes are incomplete. It has been demonstrated that f0F2 exhibits diurnal and seasonal variations remarkably [29]. The ionospheric vertical stations record a batch of observations hourly, which has twenty-four sets of data from 0 to 23. Here we chose the hour number (HR) as the index of the diurnal variation. To avoid numerical discontinuity at the midnight boundary, HR were converted to two quadrature components according to the following:

$$HRS = sin\left(\frac{2\pi \times HR}{24}\right) \tag{17}$$

$$HRC = cos\left(\frac{2\pi \times HR}{24}\right) \tag{18}$$

Not only the hour of day, but also the day of year has an effect on the variations of the f0F2, due to the response of the critical frequency to the seasonal changes in the solar X-ray radiation and solar extreme ultraviolet (EUV) radiation from the sun [30]. Similarly to the transform to hour of day, we use sine and cosine to convert the day of year (DY) as following formulas to describe the seasonal variation:

$$DYS = sin\left(\frac{2\pi \times Day}{365}\right) \tag{19}$$

$$DYC = cos\left(\frac{2\pi \times Day}{365}\right) \tag{20}$$

3.3 Solar Activity Index and Magnetic Index.

The ionospheric variations are directly affected by solar solar activity index and magnetic index, and the prediction accuracy of the recurrent neural network model would be improved by adding solar index and magnetic index to inputs. We added two more parameters into inputs as following:

• Solar activity index: solar 10.7cm radio flux, f10.7
• Magnetic index: Ap and Kp

4. Experiment and Discussion

The recurrent neural network was trained using the data sets described above. In order to examine the applicability and practicability of the RNN method, we compared the predicted results with a BPNN method and an auto-correlation method, where the input data were same in the three methods. The performance of the RNN model was evaluated by the mean absolute error (MSE) and the root mean square error (RMSE) as following:

$$\Delta f0F2 = \frac{1}{N}\sum_{i=1}^{N} |F2_o - f0F2_p| \tag{21}$$

$$RMS = \sqrt{\frac{1}{N}\sum (f0F2_o - f0F2_p)^2} \tag{22}$$

Where f0F2o and f0F2p represent the observations and the predictions in each mini-batch respectively. In the RNN model, all neural networks were trained separately for each station, which

used input data were from corresponding vertical stations. When one set of data had been processed, the RNN model generated output and then processed the testing data to verify the model accuracy. The predicted relative errors and RMS errors of test set for the RNN model, the BPNN model and the autocorrelation model were list in Table 2. By comparing three model predicted errors, it is shown that the RNN performed better than the autocorrelation and the BPNN model generally. Not surprisingly we had this epilogue, especially comparing the predicted results and the learning procedures of the RNN and the BPNN, the RNN model recorded the data of the previous time node but the BPNN did not, which mean that the performance of the RNN was much more better in the time series problems. Taking Wuhan station as an example, the RNN model had an MAE of 0.60MHz, while the MAE of the autocorrelation and the ANN were 0.65 MHz and 0.88 MHz respectively. But the computation of RNN were the biggest in these three algorithms.

Table 2 Predicted Errors of Fof2 Hourly Ahead In Rnn,Autocorrelation And Ann

Station Name	RNN		Autocorrelation		ANN	
	MAE	RMSE	MAE	RMSE	MAE	RMSE
UQ	0.25	0.41	0.40	0.58	0.62	0.89
BJ	0.32	0.56	0.49	0.67	0.65	0.96
WH	0.44	0.60	0.65	0.82	0.88	1.03
GZ	0.72	0.88	0.90	1.13	1.20	1.58
HN	0.80	1.08	1.21	1.44	1.42	1.69

Table 3 shows names and geographic coordinates of Hainan, Guangzhou, Beijing, Urumqi, and Wuhan. These five cities basically cover the whole territory of China, which are typical mid-latitude cities. Though Table 1 shows the typical mid-latitude ionospheric predictions, the impact of geographical location on the ionospheric variations still exists. Taking Urumqi and Hainan as examples (Urumqi locates in the north and Hainan locates near the equator), it is found that the forecasting errors at Urumqi station are lower than those at Hainan station, which could be explained that the ionosphere over Hainan might be affected by the Equatorial Anomaly [31] and the solar activities seriously, causing the ionospheric variations larger. And then ionospheric variability leads to the forecasting errors increasing.

Table 3 Main Observations From Ionospheric Vertical Stations

Station	Geography Latitude	Geography Longitude
UQ	87.62◦	43.82◦
BJ	116.46◦	39.92◦
WH	114.30◦	30.60◦
GZ	113.23◦	23.16◦
HN	110.35◦	20.02◦

The f0F2 has seasonal variations evidently. And in different seasons, solar activity intensity is not at the same level. Meanwhile, solar activity has an effect on the geomagnetic activity. Finally the ionosphere is influenced by solar, geomagnetic activities and seasonal changes. The division of the four seasons in China is that spring includes March, April and May, summer includes June, July and August, autumn includes September, October and November and winter includes December, January and February. And the 24th solar activity cycle ended because from January 2016 to April 2017 [32], the solar flare happened on Level M or above, and the rest of the solar activity was at low level. It is considered that 2015 was a high solar activity year, and 2016 was a low solar activity year as testing sets for the RNN model. Table 4 gives the MAE and the RMSE for for different seasons in 2015 and 2016, respectively.

Table 4 Different Seasons In High Or Low Solar Year

Station Name	Four Seasons	2015(High Year)		2016(Low Year)	
		MAE	RMSE	MAE	RMSE
UQ	spring	0.38	0.59	0.25	0.51
	summer	0.49	0.80	0.40	0.72
	autumn	0.39	0.55	0.23	0.47
	winter	0.50	0.75	0.39	0.60
BJ	spring	0.45	0.70	0.33	0.56
	summer	0.53	0.75	0.44	0.66
	autumn	0.47	0.72	0.36	0.60
	winter	0.61	0.88	0.52	0.78
WH	spring	0.56	0.70	0.40	0.60
	summer	0.66	0.82	0.53	0.77
	autumn	0.42	0.66	0.37	0.58
	winter	0.61	0.88	0.49	0.81
GZ	spring	0.62	0.79	0.49	0.68
	summer	0.88	1.01	0.79	0.95
	autumn	0.59	0.85	0.43	0.66
	winter	0.90	1.11	0.72	0.94
HN	spring	0.81	1.03	0.66	0.85
	summer	1.01	1.20	0.89	1.10
	autumn	0.77	0.92	0.53	0.73
	winter	0.97	1.15	0.78	0.94

Also, diurnal variations of the f0F2 is one of the ionospheric characteristics. The f10.7 is selected as an index to evaluate the level of the solar activity. Fig 5 shows the daily F10.7 values of the Spring Equinox, Summer Solstice, Autumnal Equinox and Winter Solstice and the month in which the four solar terms located in 2016. And then Fig 6 displays two curves of predicted values and observations at corresponding days in Fig. 5.

From Fig. 6, it is found that in spring the forecast accuracy is not satisfied in the morning and at the rest time forecasts are more accurate; in summer, the solar activity is drastic and the forecasts has the same trend with the observations; in autumn, the forecast accuracy is better than summer and in winter, the forecast accuracy is low at midnight. Generally, during the time when solar activity was intense, the ionospheric plasma changed dramatically, and it was harder to forecast the f0F2.

5. Conclusion

A new and practical forecast method for predicting the ionospheric critical frequency in one hour ahead is proposed in this work. To make it work, an RNN model with BPTT learning algorithm is used. And the data from the 24th solar activity cycle were selected to train the RNN model. The performance of the RNN model is better than the autocorrelation model and the ANN model though comparing the MAE and the RMSE

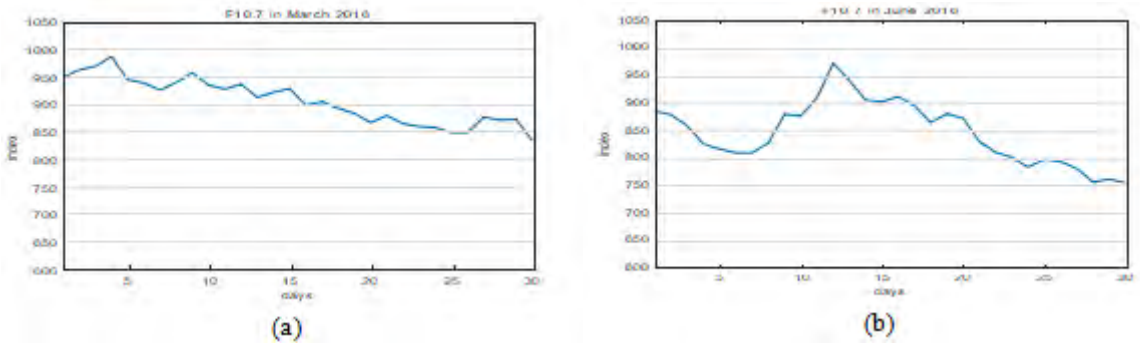

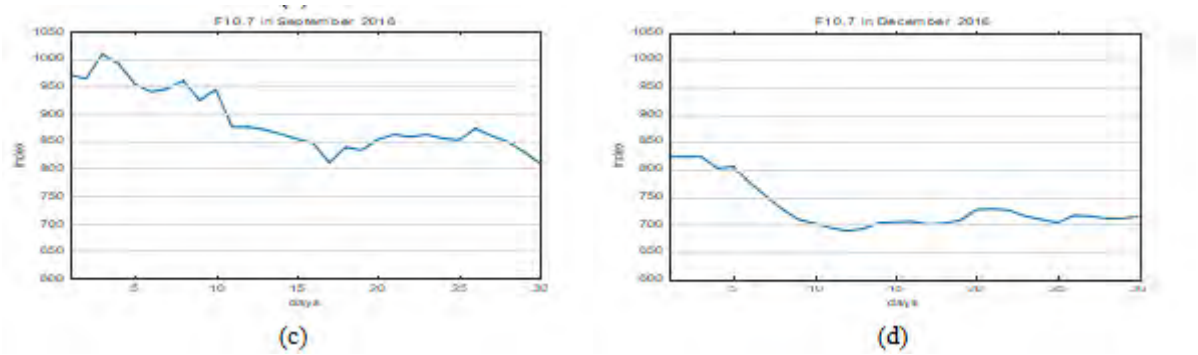

Fig. 5 (a) F10.7 in March 2016. (b) F10.7 in June 2016.
(c) F10.7 in September 2016. (d) F10.7 in December 2016.

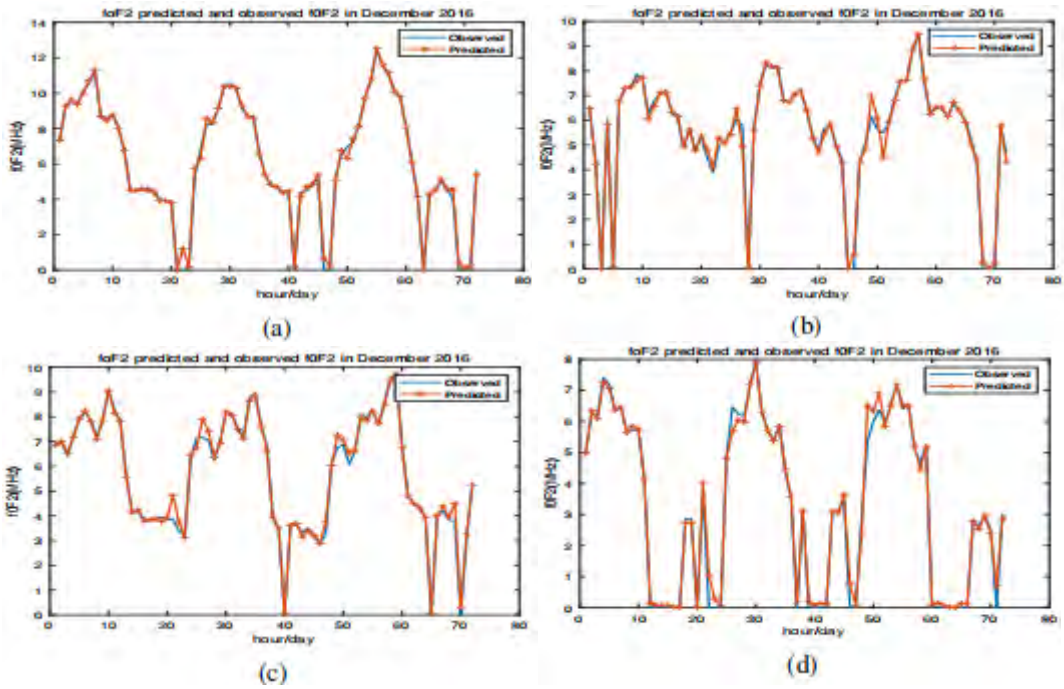

Fig. 6 (a) Description of what is contained in the first panel. (b) Description of what is contained in the second panel. (c) Description of what is contained in the second panel. (d) Description of what is contained in the second panel of three algorithms. Then the forecast results from different locations, seasons and days were discussed.

The forecasting ionospheric parameters are difficult and complicated. Owing to the RNNs outstanding performance in time series problems, we can use it not only to forecast the critical frequency of F2-layer, but also other ionospheric parameters, such as f0F1, Total Electron Content (TEC) and other complicated nonlinear values.

Acknowledgments

The National Natural Science Foundation of China under Grant 61571159 and Grant 61571157.And the datasets come from the Data Center for Geophysics, Data Sharing Infrastructure of Earth System Science, National Science & Technology Infrastructure of China.

References

[1]. Altinay.O, Tulunay.E,and Tulunay. Y. “Forecasting of ionospheric critical frequency using neural networks, “J. Geophysical Research Letters, 1997, pp.1467–1470.

[2]. Kumluca. A, Tulunay. E and Topalli. I. “Temporal and spatial forecasting of ionospheric critical frequency using neural networks, “J. Radio Science, 1999, pp. 1497–1506.

[3]. Williscroft. L.A and Poole. A. W. V. “Neural networks, foF2, sunspot number and magnetic activity, “J. Geophysical research letters, 1996, pp.3659–3662.

[4]. Lamming. X and Cander. L. R. “Monthly median foF2 modelling COST 251 area by neural networks, “J. Physics and Chemistry of the Earth, 1999, pp.349–354.

[5]. Cander. L.R, Milosavljevic. M.M, Stankovic. S.S, and Tomasevic, S. “Ionospheric forecasting technique by artificial neural network, “J. Electronics Letters, 1990, pp.1573–1574.

[6]. Francis. N. M, Cannon. P. S. and Brown. A.G. “Nonlinear prediction of the ionospheric parameter f0F2 on hourly, daily, and monthly timescales, “J. Journal of Geophysical Research: Space Physics, 2000, pp.12839–12849.

[7]. Chen. C, Wu. Z, Sun. S, Ban. P, Ding. Z. and Xu. Z. “Forecasting the ionospheric f0F2 parameter one hour ahead using a support vector machine technique, “J. Journal of Atmospheric and Solar-Terrestrial Physics, 2010, pp.1341–1347.

[8]. Chen. C, Wu. Z.S, Xu. Z.W, Sun. S.J, Ding. Z.H. and Ban. P.P. “Forecasting the local ionospheric f0F2 parameter 1 hour ahead during disturbed geomagnetic conditions, “J. Journal of Geophysical Research, 2010, pp.113–115.

[9]. Feynman. J and Gabriel. S. B. “On space weather consequences and predictions, “J. Journal of Geophysical Research: Space Physics, 2000, pp.10543–10564.

[10]. Muhtarov. P and Kutiev. I. “Autocorrelation method for temporal interpolation and short-term prediction of ionospheric data, “J. Radio Sci, 1999, pp.459-464.

[11]. Sojka. J.J, Thompson. S.R and Schunk. R.W. “Assimilation ionospheric model: development and testing with combined ionospheric campaign Caribbean measurements, “J. Radio Sci, 2001, pp.247-259.

[12]. Poole. A.W.V and Mukinnell. L.A. “On the predictability of f0F2 using neural networks, “J. Radio Sci, 2000, pp.225-234.

[13]. Roble. R. G, and Ridley, E. C. “A thermosphere ionosphere mesosphere electrodynamics general circulation model (TIMEGCM): Equinox solar cycle minimum simulations (30500 km), “J. Geophysical Research Let ters, 1994, pp.417–420.

[14]. Koutroumbas. K, Tsagouri. I and Belehaki. A. “Time series auto regression technique implemented on-line in DIAS system for ionospheric forecast over Europe, “C. Annales geophysicae: atmospheres, hydro spheres and space sciences, 2008, pp.371–375.

[15]. Koutroumbas. K and Belehaki. A. “One-step ahead prediction of f0F2 using time series forecasting techniques, “C. Annales Geophysicae, 2005, pp.3035–3042.

[16]. Tsagouri. I, Koutroumbas. K, and Belehaki, A. “Ionospheric f0F2 forecast over Europe based on an autoregressive modeling technique driven by solar wind parameters,“J. Radio Science,2009, pp.44–45.

[17]. Tsagouri. I. and Belehaki. A. “An upgrade of the solar wind driven empirical model for the middle latitude ionospheric storm time response, “J. Atmos. Solar-Terr. Phys, 2008,pp. 2061-2076.

[18]. Tsagouri. I, Koutroumbas. K and Belehaki. A. “Ionospheric f0F2 forecast over Europe based on an autoregressive modelling technique driven by solar wind parameters, “J. Radio Sci, 2009, pp.44–50.

[19]. Tsagouri. I and Belehaki. A. “A new empirical model of middle latitude ionospheric response for space weather applications, “J. Adv. Space Res, 2006, pp.420-425.

[20]. Araujo-Pradere. E.A, Fuller-Rowell. T.J. and Codrescu. M.V. “STORM: An empirical storm-time ionospheric correction model 1. Model description,“J. Radio Science, 2002, pp.1070–1075.

[21]. Araujo-Pradere. E.A, Fuller-Rowell, T.J, and Codrescu, M.V. “STORM: An empirical storm-time ionospheric correction model 2. Validation,“J. Radio Science, 2002, pp.1076–1080.

[22]. Ban. P.P, Sun. S.J, Chen. C, and Zhao. Z.W. “Forecasting of low-latitude storm-time ionospheric f0F2 using support vector machine, “J. Radio Science, 2011, pp.6008–6018.

[23]. Lecun. Y, Bengio. and Y, Hinton. G. “Deep learning,“J. Nature,2015,pp.436–456.

[24]. Lipton. Z. C, Berkowitz. J. and Elkan. C. “A Critical Review of Re current Neural Networks for Sequence Learning,“J. Computer Science, 2015,pp.102–110.

[25]. Wintoft. P and Cander. L. R. “Twenty four hour predictions of f0F2 using time delay neural networks,“J. Radio Science,2000, pp.395–408.

[26]. Khachikian. G. I, Pogorel’Tsev. A. I, and Drobzheva, I. V. “Characteristics of longitudinal variations of f0F2 at midlatitudes of the Northern Hemisphere-Dependence on local time and season, “J. Geomagnetism and Aeronomy, 1989, pp.571–576.

[27]. Cho. K, Merrienboer. B. V. and Gulcehre. C. “Learning Phrase Representations using RNN Encoder-Decoder for Statistical Machine Trans lation, “J. Computer Science, 2014, pp.34–46.

[28]. Mao. J, Xu. W and Yang. Y. “Deep Captioning with Multimodal Recur rent Neural Networks (m-RNN), “J. Eprint Arxiv, 2015, pp.1025–1035.

[29]. Kazimirovsky. E. S. and KoKouRov. V. D. “The tropospheric and stratospheric effects in the ionosphere, “J. Journal of geomagnetism and geoelectricity, 1991, pp.551–562.

[30]. Liu. L. B, Wan. W. X and Chen. Y. D. “Solar activity effects of the ionosphere: A brief review, “J. Chinese Science Bulletin, 2011, pp.1202–1211.

[31]. Anderson. D. N. “A theoretical study of the ionospheric F region equatorial anomaly I. Theory. “J. Planetary and Space Science, 1973, pp.409–419.

[32]. Ballester. J. L, Oliver. R and Carbonell. M. “Return of the near 160 day periodicity in the photospheric magnetic flux during solar cycle 23, “J. The Astrophysical Journal Letters, 2004, pp.173–185.